

B Physics at CDF

Elisa Pueschel (on behalf of CDF Collaboration)

Carnegie Mellon University

Abstract. We present the latest B physics results from the CDF experiment at the Fermilab Tevatron collider. We focus on a number of analyses, including a measurement of the forward-backward asymmetry of $B \rightarrow K^{(*)}\mu\mu$ decays, determination of the CP violating phase $\sin 2\beta_s$ in $B_s^0 \rightarrow J/\psi\phi$ decays, $B \rightarrow J/\psi X$ lifetime measurements, observation of resonance structure in $\Lambda_b \rightarrow \Lambda_c \pi^- \pi^+ \pi^-$, and $\Upsilon(1S)$ polarization.

1. Introduction

The Tevatron is a $p\bar{p}$ collider, with collisions occurring at 1.96 TeV center of mass energy. As a hadron collider, the Tevatron has access to all bottom species, including B^0 , B^+ , B_s^0 , B_c^+ and Λ_b^0 hadrons. The hadronic detector environment is complex, with large amounts of background. The CDF experiment employs sophisticated triggers to select B decays. Additionally, CDF's precise momentum and vertexing resolution facilitate a variety of B physics measurements, ranging from lifetime and CP violation studies to B hadron spectroscopy measurements.

2. Forward-backward asymmetry in $B \rightarrow K^{(*)}\mu\mu$

Flavor changing neutral current processes can occur via penguin diagrams in the standard model. The transition $b \rightarrow s\ell\ell$, for instance, is a FCNC process, present in the decays $B^+ \rightarrow K^+\mu^+\mu^-$, $B^0 \rightarrow K^{*0}\mu^+\mu^-$ and $B_s \rightarrow \phi\mu^+\mu^-$. The rates for these decays could be enhanced by new physics contributions to the penguin diagrams. This would consequently alter the differential branching ratio and forward-backward asymmetry for these decays from the standard model predictions.

$B^+ \rightarrow K^+\mu^+\mu^-$, $B^0 \rightarrow K^{*0}\mu^+\mu^-$ and $B_s \rightarrow \phi\mu^+\mu^-$ decays are reconstructed using 4.4 fb^{-1} of data from a di-muon trigger. The observed signal yields for the three decay modes are 120 ± 16 , 101 ± 12 , and 27 ± 6 events, respectively. This measurement is the first observation of $B_s \rightarrow \phi\mu^+\mu^-$ decays at a 6.3σ significance. The absolute branching ratios of the three modes are measured to be: $BR(B^+ \rightarrow K^+\mu^+\mu^-) = 0.38 \pm 0.05(\text{stat}) \pm 0.03(\text{syst}) \times 10^{-6}$, $BR(B^0 \rightarrow K^{*0}\mu^+\mu^-) = 1.06 \pm 0.14(\text{stat}) \pm 0.09(\text{syst}) \times 10^{-6}$, $BR(B_s^0 \rightarrow \phi\mu^+\mu^-) = 1.44 \pm 0.33(\text{stat}) \pm 0.46(\text{syst}) \times 10^{-6}$.

The differential branching ratio for the $K^{(*)}$ modes was measured in bins of $q^2 = M_{\mu\mu}^2$, as shown in Figure 1. The limits on the standard model expectation are denoted by the red lines. The data points are consistent with these limits.

The K^{0*} polarization F_L and $B^0 \rightarrow K^{0*}\mu^+\mu^-$ and $B^+ \rightarrow K^+\mu^+\mu^-$ forward-backward asymmetry A_{FB} are also measured. An angular analysis is performed to extract F_L and A_{FB} in bins of $q^2 = M_{\mu\mu}^2$. Results are shown in Fig. 2. The standard model expectation is denoted by a red line, and a generic new physics scenario with flipped sign of the Wilson coefficient C_7 is indicated by a blue line. The precision of the measurement is not adequate to determine which scenario is favored. The results are consistent and competitive with B factory measurements [1].

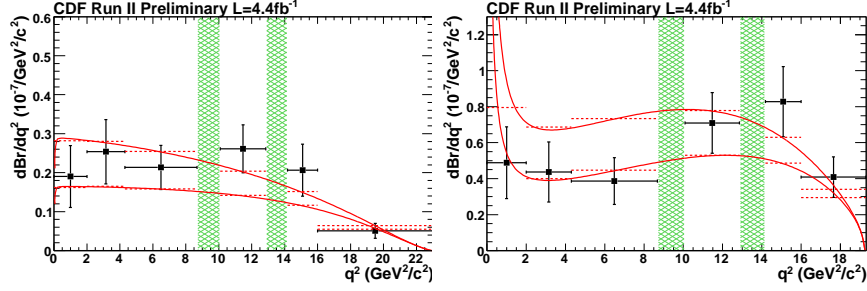


Figure 1. Differential branching ratio for $B^+ \rightarrow K^+ \mu^+ \mu^-$ (left) and $B^0 \rightarrow K^{*0} \mu^+ \mu^-$ (right). The limits for the standard model expectation are shown in red.

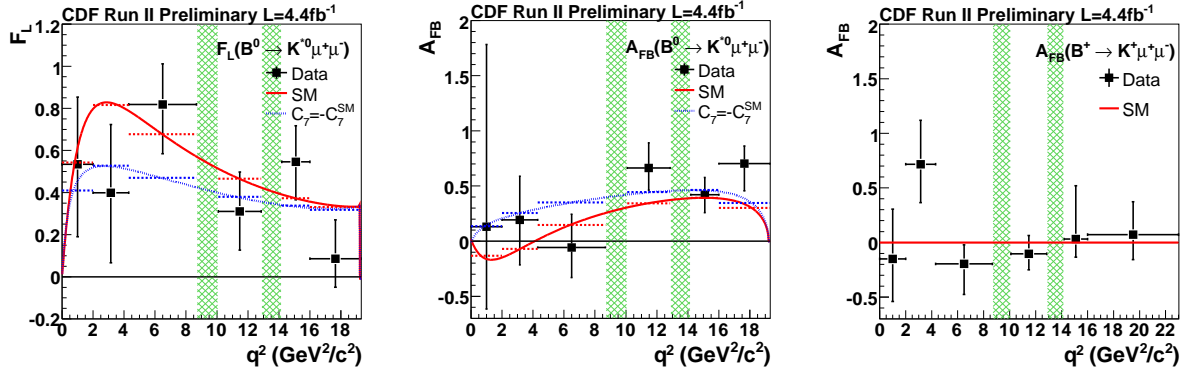


Figure 2. K^{0*} polarization F_L and $B^0 \rightarrow K^{0*} \mu^+ \mu^-$ and $B^+ \rightarrow K^+ \mu^+ \mu^-$ forward-backward asymmetry A_{FB} .

3. Measurement of CP violating phase $\sin 2\beta_s$ in $B_s^0 \rightarrow J/\psi \phi$ decays

The CP violating phase $\sin 2\beta_s$ quantifies the CP violation in the interference between the amplitudes from $B_s^0 \rightarrow J/\psi \phi$ and $B_s^0 \rightarrow \bar{B}_s^0 \rightarrow J/\psi \phi$ decays. In the latter case, the B_s^0 mixes into its antiparticle before decaying, through the exchange of W bosons and off-shell up type quarks in a mixing box diagram. The standard model expectation for $\sin 2\beta_s$ is small, but new physics participation in the B_s^0 mixing box diagram could result in a large value for $\sin 2\beta_s$.

The measurement is made on 2.8 fb^{-1} of data collected using the di-muon trigger. Approximately 3000 $B_s^0 \rightarrow J/\psi \phi \rightarrow \mu^+ \mu^- K^+ K^-$ events are reconstructed. An un-binned maximum likelihood fit to mass, lifetime, and final state angular distributions is used to extract $\sin 2\beta_s$. The measurement's power is enhanced by using flavor tagging algorithms, which determine whether the candidate meson was a B_s^0 or a \bar{B}_s^0 at production.

The left plot in Fig. 3 shows a confidence region in β_s and $\Delta\Gamma$ space, where $\Delta\Gamma$ is the decay width difference between the light and heavy B_s^0 mass eigenstates. The standard model expectation lies within the 95% confidence level, with a p-value of 7%. This means that the probability the true value is the standard model expectation and the observed data are a fluctuation is 7% [2].

The CDF measurement has been combined with an analogous measurement from the DØ experiment. The result is shown in the right plot in Fig. 3. The standard model expectation falls outside the 95% confidence level, indicating a 2σ deviation of the contours from the SM prediction [3].

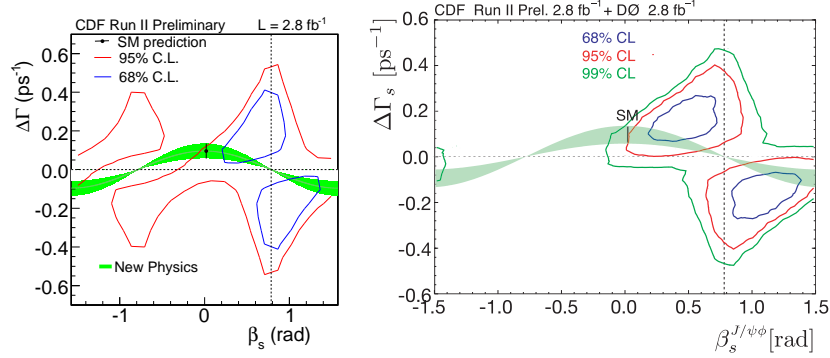


Figure 3. $\beta_s - \Delta\Gamma$ confidence region, CDF only (left), Tevatron combined result (right). The green bands show the allowed region assuming mixing-induced CP violation.

4. $B \rightarrow J/\psi X$ lifetimes

The measurement of B meson lifetimes is an important test of heavy quark effective theory. The B^+ , B^0 , and Λ_b^0 lifetimes are measured using 4.3 fb^{-1} of data collected with the CDF di-muon trigger. For $B^+ \rightarrow J/\psi K^+$, $45,000 \pm 230$ events are reconstructed, for $B^0 \rightarrow J/\psi K^{*0}$, $16,860 \pm 140$ events, for $B^0 \rightarrow J/\psi K_s^0$, $12,070 \pm 120$ events, and for $\Lambda_b^0 \rightarrow J/\psi \Lambda^0$, $1,710 \pm 50$ events.

A combined fit to mass and lifetime is used to determine the lifetime. The fit projection for the mass is shown in the left-most plot in Fig. 4. The fit projections for proper time and its error in the signal region are shown in the center and right-most plots.

The lifetimes, which are the world's best measurements, are the following [4]:

- $\tau(B^+) = 1.639 \pm 0.009(\text{stat}) \pm 0.009(\text{syst}) \text{ ps}$
- $\tau(B^0) = 1.507 \pm 0.010(\text{stat}) \pm 0.008(\text{syst}) \text{ ps}$
- $\tau(\Lambda_b^0) = 1.537 \pm 0.045(\text{stat}) \pm 0.014(\text{syst}) \text{ ps}$
- $\tau(B^+)/\tau(B^0) = 1.088 \pm 0.009(\text{stat}) \pm 0.004(\text{syst})$
- $\tau(\Lambda_b^0)/\tau(B^0) = 1.020 \pm 0.030(\text{stat}) \pm 0.008(\text{syst})$.

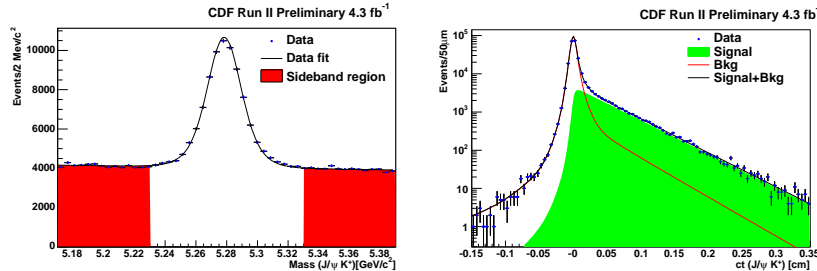


Figure 4. Fit projections for mass (left) and proper time (right).

5. Resonance structure of $\Lambda_b^0 \rightarrow \Lambda_c^+ \pi^- \pi^+ \pi^-$

The Λ_b^0 meson can decay to an intermediate resonant states before decaying to the final state $\Lambda_c \pi^- \pi^+ \pi^-$. This measurement is the first observation of these decay modes and their relative branching fractions.

The measurement is performed on 2.4 fb^{-1} of data, collected using the two-track trigger. The following resonant modes are observed, with yields:

- $\Lambda_b^0 \rightarrow \Lambda_c(2595)^+ \pi^- \rightarrow \Lambda_c^+ \pi^- \pi^+ \pi^-$, 46.6 ± 9.7 events
- $\Lambda_b^0 \rightarrow \Lambda_c(2625)^+ \pi^- \rightarrow \Lambda_c^+ \pi^- \pi^+ \pi^-$, 114 ± 13 events
- $\Lambda_b^0 \rightarrow \Sigma_c(2455)^{++} \pi^- \pi^- \rightarrow \Lambda_c^+ \pi^- \pi^+ \pi^-$, 81 ± 15 events
- $\Lambda_b^0 \rightarrow \Sigma_c(2455)^0 \pi^+ \pi^- \rightarrow \Lambda_c^+ \pi^- \pi^+ \pi^-$, 41.5 ± 9.3 events
- $\Lambda_b^0 \rightarrow \Lambda_c^+ \rho^0 \pi^- + \Lambda_c^+ 3\pi(\text{other}) \rightarrow \Lambda_c^+ \pi^- \pi^+ \pi^-$, 610 ± 88 events.

The relative branching fractions are as follows [5]:

- $\frac{BR(\Lambda_b^0 \rightarrow \Lambda_c(2595)^+ \pi^- \rightarrow \Lambda_c^+ \pi^- \pi^+ \pi^-)}{BR(\Lambda_b^0 \rightarrow \Lambda_c^+ \pi^- \pi^+ \pi^- (\text{all}))} = 2.5 \pm 0.6(\text{stat}) \pm 0.5(\text{syst}) \times 10^{-2}$
- $\frac{BR(\Lambda_b^0 \rightarrow \Lambda_c(2625)^+ \pi^- \rightarrow \Lambda_c^+ \pi^- \pi^+ \pi^-)}{BR(\Lambda_b^0 \rightarrow \Lambda_c^+ \pi^- \pi^+ \pi^- (\text{all}))} = 6.2 \pm 1.0(\text{stat})_{-0.9}^{+1.0}(\text{syst}) \times 10^{-2}$
- $\frac{BR(\Lambda_b^0 \rightarrow \Sigma_c(2455)^{++} \pi^- \pi^- \rightarrow \Lambda_c^+ \pi^- \pi^+ \pi^-)}{BR(\Lambda_b^0 \rightarrow \Lambda_c^+ \pi^- \pi^+ \pi^- (\text{all}))} = 5.2 \pm 1.1(\text{stat}) \pm 0.8(\text{syst}) \times 10^{-2}$
- $\frac{BR(\Lambda_b^0 \rightarrow \Sigma_c(2455)^0 \pi^+ \pi^- \rightarrow \Lambda_c^+ \pi^- \pi^+ \pi^-)}{BR(\Lambda_b^0 \rightarrow \Lambda_c^+ \pi^- \pi^+ \pi^- (\text{all}))} = 8.9 \pm 2.1(\text{stat})_{-1.0}^{+1.2}(\text{syst}) \times 10^{-2}$

6. $\Upsilon(1S)$ Polarization

Measurements of the J/ψ and $\Upsilon(1S)$ polarization are used to test the predictions of non-relativistic QCD. The J/ψ polarization measurement disagrees with theory, making $\Upsilon(1S)$ polarization the subject of much interest.

The measurement is made on 2.9 fb^{-1} of data, collected with a di-muon trigger. The polarization parameter α is determined by studying the distribution of the angle $|\cos(\theta^*)|$ associated with the positive muon from $\Upsilon(1S) \rightarrow \mu^+ \mu^-$. By comparing the observed angular distributions in different $p_T(\Upsilon)$ bins with templates of fully transverse and longitudinal Monte Carlo (as shown in the left plot in Fig. 5), the polarization can be determined. The polarization parameter α is shown as a function of p_T in the right plot in Fig. 5, with the NRQCD prediction in green. The data are in poor agreement with theory at high p_T [6].

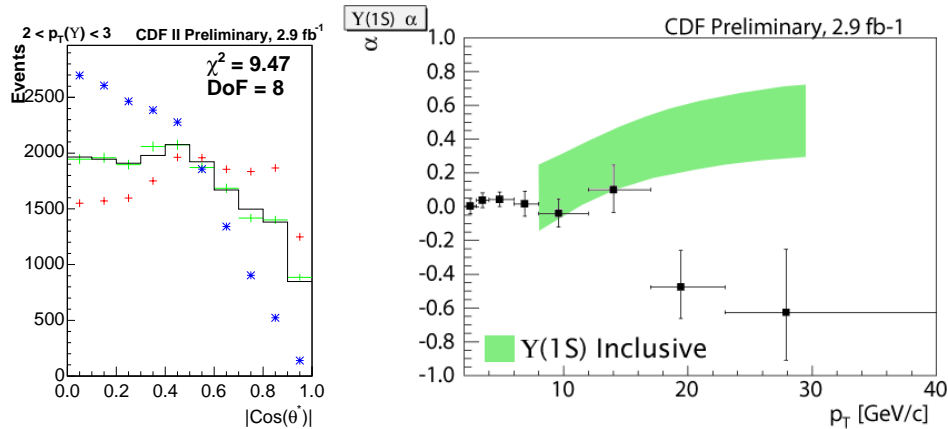


Figure 5. Polar angle distribution for μ^+ with transverse (red) and longitudinal (blue) Monte Carlo templates (left). Polarization as a function of p_T , with NRQCD predictions (green).

- [1] T. Aaltonen et. al (CDF collaboration), CDF note 10047 (2010)
- [2] T. Aaltonen et. al (CDF collaboration), CDF note 9458 (2008)
- [3] T. Aaltonen et. al (CDF collaboration), CDF note 9787 (2009)
- [4] T. Aaltonen et. al (CDF collaboration), CDF note 10071 (2010)
- [5] T. Aaltonen et. al (CDF collaboration), CDF note 10001 (2009)
- [6] T. Aaltonen et. al (CDF collaboration), CDF note 9966 (2009)